CFSRC COLLOQUIUM

Proceedings of the Cold-Formed Steel Research Consortium Colloquium
17-19 October 2022 (cfsrc.org)

Influences of cold working on tensile and bending strength of cold roll formed steel sections contain complex folded-in stiffeners

S.J. Qadir[1], V.B. Nguyen[2], I. Hajirasouliha[3], M.A. English[4]

Abstract

This paper aims to study the cold working influences on material and structural properties of the cold roll formed steel sections contain complex longitudinally stiffeners under bending. Tensile tests on flat and curved samples extracted from the complex stiffeners of channel and zed sections were conducted to investigate the change of material properties due to cold working during the roll forming process. The influences of cold working in the section flat regions, corners and stiffener bends were investigated and evaluated against some predictive models in literature studies. Nonlinear Finite Element modelling was developed to model the four-point bending tests to study the effects of cold working on the buckling and ultimate strengths of channel and zed sections. In the bending models, experimental material properties of section flat parts, corners and stiffener bends were implemented to search for the optimal shapes of the sections. Significant improvements were obtained for the section strength of the optimized sections in comparison to the original sections. Optimal shapes for the channel and zed sections with maximum strength in distortional buckling could be obtained while changing the stiffeners' position, shape, sizes, and considering the effect of cold working. It revealed that, the optimal sections provided up to 13% and 17% increase in bending strength for the channel and zed section, respectively; however, when the effect of cold working at the section corner and the stiffener's bend regions was included, the increase in bending strength increased up to 20% and 23%, respectively.

1. General

Cold-formed steel (CFS) members are manufactured by cold rolled forming or press braking processes. In both methods, steel sheet or strip, which would generally have been cold rolled formed, serves as the feed material. The cold rolled forming is generally a most advanced process by which steel strip (virgin coil material) is passed through a series of rollers arranged in tandem that progressively form the strip into the final cross-sectional shape. Different levels of cold working or plastic deformation in material are generated during the section forming process, resulting in changes to the mechanical properties of the virgin coil material. The varying level of cold working induced at different positions around the section is often seen in the cold roll formed sections and significant levels of cold working are found in the regions around section corners and stiffeners' bends.

Several studies have been carried out to quantify the cold working effects in the curved regions of metallic material and developed a number of models to predict the strength enhancement. The most widely used of which are for the stainless-steel sections [1-8] and the CFS sections [9-11]. Karren [9] carried out investigations into the cold working effects in the curved regions of CFS sections and suggested a model to determine the yield strength enhancement in the section corners. This model is currently used for the Design of Cold-formed Steel Structural Members included in the AISI Specification [12]. Abdel-Rahman and Sivakumaran [10] performed extensive tensile specimen tests for CFS channel sections and found that the cold working effects also exist in the area adjacent to the corners despite that these are not as significant as in the curved corner areas themselves. They proposed a modification for the Karren's model to consider the average increased yield strength within the corner zone. Gardner et al. [11] also carried out tensile tests extracted from the flat and corner regions of the CFS hollow sections. They observed that the tensile strength results obtained from the Karren's model overestimated the tensile test results and therefore proposed a new model (based on the modification in the Karren's model); they found that the new proposed model provided more consistent and accurate corner yield strength predictions than those obtained from the Karren's model for cold-formed rectangular and square hollow sections.

[1] Lecturer, Department of Civil Engineering, University of Sulaimani, sangar.qadir@univsul.edu.iq
[2] Associate professor, Department of Mechanical and Built Environment, University of Derby, vb.nguyen@derby.ac.uk
[3] Associate professor, Department of Civil and Structural Engineering, University of Sheffield, i.hajirasouliha@sheffield.ac.uk
[4] Engineer, Hadley Industries plc, Smethwick, West Midlands, B66 2PA, United Kingdom, martin.english@hadleygroup.com

Several studies have investigated the cold formed sections, where the cold working effects on mechanical properties of the material and their effects on structural behavior of the sections were quantified. Some studies measured the strength enhancement in the section corners and pointed out that it had negligible effect on load-carrying capacity of structural column members [13-15]. Other studies, however, have shown the cold working effects had significant influence on load carrying capacity of structural column members [4, 16-21] and beam member [22].

In addition to the cold working effects on strength and behavior of CFS structural members, the optimization of predefined orthodox CFS cross-sections have been widely performed by previous researchers to optimize channel, zed and sigma sections in order to optimize the relative dimensions of the sections, which they have been primarily focused on using analytical formulas or the methods available in the Codes and Specifications such as AISI-S100 Specification [12] and Eurocode 3 (EC3) [23] (i.e. the Effective Width Method and the Direct Strength Method in calculating the elastic buckling, compression and flexural strength of the structural members. Most of these design methods available in the design guidelines [12, 23] used the Effective Width Method for strength determination. This method is often applicable for conventional sections which fall within the dimensional limits of the design standard and a clear distinction between flanges, web and lips can be made.

An alternative method has been used by combining the Finite Strip Method and the Direct Strength Method in some of the recent optimization studies of CFS structural beam members [36-38]. The elastic critical local, distortional, and global buckling stresses can be calculated by the DSM to obtain the strength capacity. The DSM can therefore, in principle, be used to calculate the strength of any shape in which FSM analysis is often used to obtain the elastic buckling stresses of the sections. Some shortcomings, however, have been seen in this method. The DSM equations were developed based on the statistical correlation between a cross-sectional slenderness parameter and the ultimate strength capacity. This can make the DSM predictions significantly cross-sectional dependent and may exhibit a significant coefficient of variation, resulted in predicting less accurate strength capacity for certain cross sections. In addition, distortional-global or local-distortional interactions cannot be obtained from the DSM equations [24]. This can be significantly problematic as reported optimization results may not be correctly predicted.

It is noted that the current design methods [12, 23] are very limited in their ability to evaluate the strength of unorthodox cross-sectional shapes that include channel and zed sections contain complex folded-in stiffeners. On the other hand, most of previous studies on the optimization of CFS sections did not consider the effect of both the geometry and the cold working effects on the strength of the section, resulting in not very accurate results. Only the recently published studies [25, 26] used FE modelling and optimization techniques to investigate the influences of cold working at the section corners and stiffener bends and the stiffeners' size, shape and location during the manufacturing process. However, in these studies, the tests were not carried out to obtain the material properties of corners and bends, but the North American specification [12] formulae were used to obtain the material properties based on the flat regions of the sections. While providing useful information on the effect of geometric shape and cold working by the cold roll forming process on the strength of sections with complex stiffeners, it did not provide accurate figures on the cold working effects on material properties and on structural behavior of these sections. In addition, there has not been any experimental investigations on the effects of cold working on complex stiffener shapes.

Therefore, the work in this study is driven by the need to explore the influence of cold working effects on mechanical properties and flexural strength of the cold roll formed sections with complex stiffener shapes by experimental testing and by numerical modelling and optimization techniques. A tensile test programme on cold roll formed structural longitudinally stiffened sections, including channel and zed sections was conducted. The cold working effects in the section corner and stiffener bend regions of cold roll formed sections was analyzed and the applicability of existing predictive models was evaluated. The four-point bending tests were modelled using nonlinear Finite Element modelling to study the flexural strength of channel and zed sections with complex stiffeners. The material properties at section flat parts, corners and stiffener bends obtained from the tensile tests were used for the sections to accurately study the effects of cold working on the section strengths. Optimization techniques using FE modelling and response surface optimization were implemented to search for the optimal shapes of the sections. Optimal cross-sectional shapes of the longitudinally stiffened channel and zed sections were finally selected and proposed.

2. The cold working effects on mechanical properties of cold roll formed sections

2.1 Tensile tests

96 tensile specimens obtained from 4 different channel and zed sections were tested. The tensile specimens were extracted from channel and zed sections with complex stiffeners. The channel and zed sections had material properties and geometries which were similar to some channel and zed sections that were already conducted in the bending tests in the previous studies [27]. The relationship

between these sections were specified in detail in Section 2.3. The zed section label begins with Z whereas the channel section begins with C. For instance, a section labelled as Z-W200T2.0 represents as follows: Z: zed section; W: Web, 200 Nominal web height or section depth (mm); T: Thickness, 2.0: Nominal plate thickness (mm). The section's geometries and dimensions, which the tensile test specimens were taken, are summarized in Table 1.

Table 1: The section's geometries and measured dimensions where the tensile test specimens were taken.

Sample section	Thickness (mm)	Depth (mm)	Top flange (mm)		Bottom flange (mm)	
			Width	Lip	Width	Lip
Z-W200T2.0	1.95	200.01	70.01	15.02	60.02	13.01
Z-W145T1.2	1.24	145.06	67.00	15.02	61.02	13.93
C-W200T2.0	1.99	200.01	63.02	16.01	63.02	16.01
C-W145T1.2	1.22	145.01	63.05	16.02	63.05	16.02

The material properties of flat and curved specimens extracted from the flat parts, corners and stiffener bends of cold roll formed steel section samples were obtained from tensile tests. The tensile specimens were extracted in channel and zed sections, and in each type, they were grouped depending upon the locations and thicknesses. The center of the web / flange plates in the longitudinal direction of the finished sections were used to obtain the tensile specimens. The same coil material prior to section roll forming were used to extract the tensile specimens. Flat and curved steel specimens had the 'dog bone' shape and were prepared according to the appropriate specifications of the relevant European standard ISO 6892-1 (ISO 2009). The flat specimens had a nominal width of 12.5 mm, while the curved specimens had different widths depending on the positions and sizes of the cross sections, ranging from 3.5 to 12.5 mm. The positions of the extracted specimens from the selected sections (Table 1) are shown in Fig. 1. The specimen identification system begins with the specimen type, followed by the specimen locations labelled as a, b, c, d and, finally, for repeated tests, the specimen test numbers 1, 2, 3 in front of specimen locations a, b, c, d, as shown in Fig. 1.

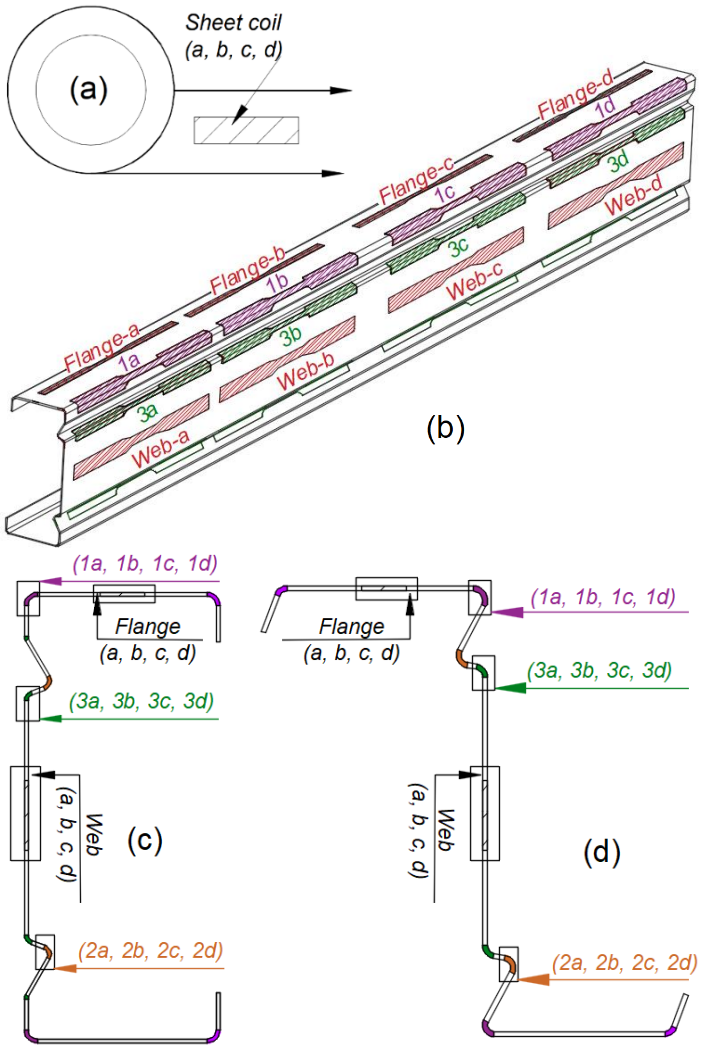

Figure 1: Locations of extracted tensile specimens (a) sheet coil prior to cold roll forming process, (b) longitudinal channel section, (c) channel cross-section, and (d) zed cross-section.

The dimensions measurement was carried out for each specimen before testing. The initial cross-sectional area was calculated from the width and thickness for the flat specimens, measured using a micrometer. The reversed lens technique was used to take a macro photograph of the cross section for the curved specimens, as illustrated in Fig. 2. The photos were then transferred into AutoCAD software and scaled to the real dimensions. The measured width of the specimen along the gauge length was then superimposed on the photograph, allowing the area to be calculated using the same software. A maximum difference in the calculated areas of less than 1% was observed for all specimens by repeating the process with pictures taken from the other end of the specimen. The calculated area was then used to calculate stress from the measured force divided by the area and the strain was obtained from the strain gauges and the extensometer measurements.

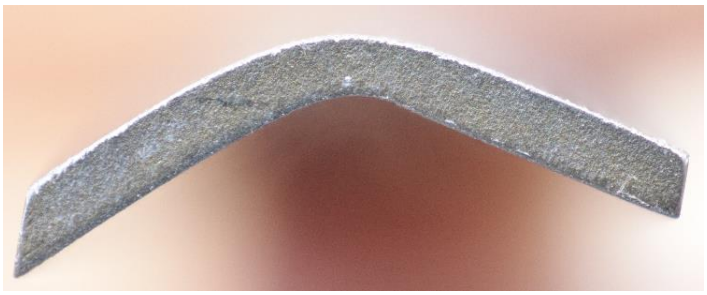

Figure 2: Macro photograph of a typical curved cross section at the gripped end of the tensile specimen.

All tensile specimens were instrumented with an extensometer of 50 mm gauge length. In addition, each flat specimen was instrumented with one linear 10-mm strain gauge on each side of the specimen at mid-length to the center of both faces of each specimen using TML strain gauge adhesive of CN series (Tokyo Measuring Instruments Laboratory Co., Ltd.) to measure the strains in the initial part of the stress-strain curve, while each curved specimen was instrumented with a 10-mm linear strain gauge on the outside of the corner. Due to the asymmetric shape of the curved specimens, they were tested in pairs with a round bar with special knurled surfaces (Mitutoyo center punch set) placed between the gripped ends of the specimens, as illustrated in Figs. 3 and 4. The paired specimen arrangement avoided the need to flatten the specimen ends, which could have introduced unwanted bending moments into the specimens.

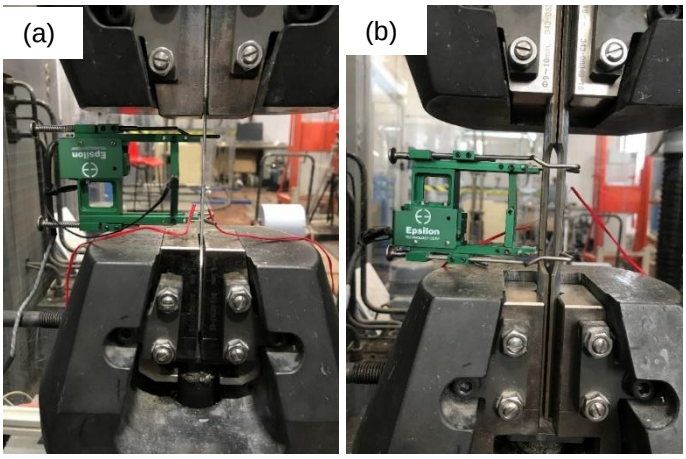

Figure 3: Typical tensile test setup (a) flat specimens and (b) curved specimens.

The tensile specimens were tested in a 300-kN Shimadzu AGS-X (Kyoto, Japan) universal testing machine, while applying a displacement rate of 1 mm/min. The strain gauge readings are more accurate comparing with the readings obtained from the extensometers, but for a much smaller range. The resulting stress-strain curves were plotted, and the yield stress was obtained at a strain level of 0.2%, while the important material property, initial Young's modulus, was determined by the readings obtained from strain gauges.

Figure 4: Typical curved specimens wired cutting from the section, Z-W200T2.0 and specimens extracted from curved locations 1a, 1b, 1c, 1d and the associated gripped inserts (a), and the test specimens before and after testing with attached strain gauges (b).

2.2 Predictive models

The influence of cold working on mechanical properties of curved regions of a cold formed section generally depended on some parameters such as : (1) the ratio of the ultimate

tensile strength f_u to the yield strength f_y of the virgin material, (2) the ratio of the inner corner radius r_i to the thickness of the steel plate t, (3) the steel grade, (4) the type of manufacturing processes (roll forming or press-braking), (5) the type of stresses (compression or tension), and (6) the direction of stress with respect to the direction of cold working, i.e. transverse or longitudinal directions [9,12]. Among the above parameters, the ratios of f_u/f_y , r_i/t, and the type of manufacturing processes were the most important parameters to influence the change of material properties during manufacturing process. For instance, the effect of cold working on the enhancement of the yield strength increased when the ratio of f_u/f_y increased. Small ratio of r_i/t, corresponded to a large degree of cold working in a corner which resulted the greater the enhancement in yield strength.

In this paper, the influence of cold working on mechanical properties of the material of different section geometries were investigated using experimental tensile testing for 4 different sections. These sections had almost the same ratio of the inner corner radius r_i to the thickness of the steel sheet t, r_i/t. For example, the inner corner radius r_i of location 1 of the zed section Z-W145T1.2-1 was 2.381 mm and the thickness of the steel sheet t was 1.259 mm, resulting in a ratio r_i/t of 1.89. For the zed section Z-W200T2.0-1, the inner corner radius r_i of location 1 was 4.366 mm and the thickness of the steel sheet t was 1.934 mm, resulting in a ratio r_i/t of 2.26. From these, it showed that as the section's dimensions increased from section Z-W145T1.2 to section Z-W200T2.0, both the inner corner radius r_i and the thickness t increased accordingly, however, the ratio of r_i/t was almost unchanged. The parameters most affected by the cold working was found to be the steel grade and the ratio of the ultimate tensile strength f_u to the yield strength f_y of the virgin material. Therefore, in this paper these two parameters were used to conduct further investigations as shown in Section 5.3.2.

Analytical methods could be applied to determine the material properties at corners and stiffener's bends affected by the cold working from the material properties of virgin coil material. One of the most popular methods was using formulae from the North American specification [12] for cold-formed steel structural members which is presented here. The equation for determining the tensile yield strength, f_{yc}, of the corner was based on the equation (1) which was empirically derived from tests by Karren [9]. The equations (1-3) are referred to hereinafter as the AISI Specification [12].

$$F_{yc} = \frac{B_c F_{yv}}{\left(\frac{R}{t}\right)^m} \qquad (1)$$

In which

$$m = 0.192\frac{F_{uv}}{F_{yv}} - 0.068 \qquad (2)$$

$$B_c = 3.69\frac{F_{uv}}{F_{yv}} - 0.819\left(\frac{F_{uv}}{F_{yv}}\right)^2 - 1.79 \qquad (3)$$

Where: F_{yv} and F_{uv} are yield stress and ultimate strength of the flat region material, R is inside corner radius and t is the plate thickness.

The strength enhancement in the corner regions of cold-formed steel sections is dependent on two main parameters based on the AISI Specification such as (i) the potential for cold-working represented by the ratio of the ultimate tensile strength f_u to the yield strength f_y of the virgin material, and (ii) the induced level of plastic strain presented by the ratio of the inner corner radius r_i to the thickness of the steel sheet t. Note that values of f_u and f_y are provided in mill certificates but the values given in material specifications should be adopted for design purposes.

Based on test results on corner material extracted from cold-formed steel box sections, Gardner et al. [11] changed the predictive model available in the AISI Specification [equations (2), (3)], and the revised values of coefficients are provided in equations (4), (5). More accurate and consistent corner yield strength predictions found from the modified predictive model compared to those obtained from the AISI Specification for cold-formed rectangular and square hollow sections.

$$m = 0.23\frac{F_{uv}}{F_{yv}} - 0.041 \qquad (4)$$

$$B_c = 2.9\frac{F_{uv}}{F_{yv}} - 0.752\left(\frac{F_{uv}}{F_{yv}}\right)^2 - 1.09 \qquad (5)$$

In this paper, the tensile test results obtained in the current study for section corners and stiffener bends were compared to the above two models and the results are presented in Section 5.2 to evaluate the predictive model's accuracy.

2.3 Bending tests

This section provides a summary of the reference bending test programme reported previously [27]. The tested zed and channel sections had cross section shapes with two stiffeners located at the same distance from the centre of the web as illustrated in Fig. 1. The test configuration for these sections consisted of a pair of long channel or zed sections placing in parallel with a specified central span of two loading points (varied from 765 mm to 1425 mm, depending on section's depths). To approximately reflect their configurations in real applications, the four-point bending testing setup including the lateral braces was conducted. The top and bottom flanges of two specimens were attached by the steel angles 45x45 mm symmetrical to the mid-span. The steel angles provided the minimum length required to generate distortional buckling results that were not boundary condition dependent. The investigations included a total of 20 different shapes of channel and zed sections. Three different thicknesses that ranged from 1.20 mm to 3.05 mm were tested for each section with the same depth to cover a wide popular range of section slenderness used in building

construction. A total of 116 tests was conducted for both sections including four duplicated tests for each section. To prevent lateral torsional buckling, bracings with small angles of 45 × 45 mm attached to the bottom and top of the section flanges were provided, which was used to replicate the bracing distance applied in practical applications. More detailed information about the experimental testing program of bending tests were presented in Nguyen et al. [27]. The experimental bending test results with their FE modelling results are presented for validation purpose in Section 5.3.1.

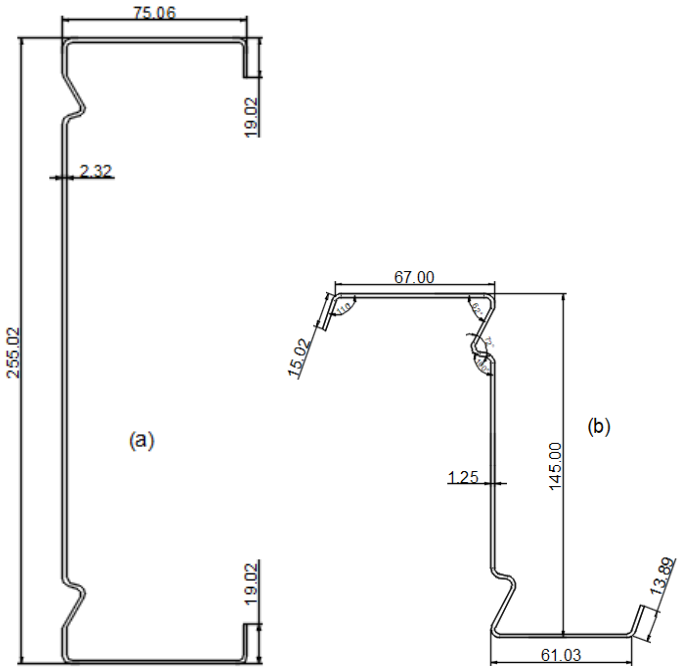

Figure 5: The cross sections and dimensions (in mm) used in experimental bending tests (a) channel section, and (b) zed section.

3. Finite Element modelling and optimization

Qadir et al. [25] developed FE models capable of simulating the buckling and ultimate bending strength of cold roll formed sections. Their FE models, which were developed in ANSYS (ANSYS, Inc.) and verified against earlier experimental testing [27], were used to calculate buckling and ultimate bending strength in this paper. Amongst many sections tested in four-point bending configuration, some were selected for conducting FEA simulations and validation. It should be noted that there were not tensile test data for corners and bends of the zed and channel section used in the bending test simulations reported previously [27]. Therefore, in this paper, the material properties obtained from tensile tests for channel section C-W200T2.0 and zed section Z-W145T1.2 presented in Table 1 were used for some sections in FEA simulations as they came from similar sources of materials (by comparing their yield and tensile strengths for the virgin coil material) and roll formed into similar section's shape and dimensions. This allowed the effects of cold working on tensile and flexural strengths of cold roll formed steel sections with complex stiffeners to be investigated using both experimental test data and predictive models, as specified in Section 2.

For the zed sections, tested sections which had similar material properties to section Z-W145T1.2 (Table 1) were selected. They had nominal dimension as follows: a thickness of 1.2 mm, a depth of 145 mm, top flange's width of 67 mm and lip length of 15 mm, bottom flange's width of 61 mm and lip length of 14 mm, and tested in the bending test under a pair of 2295 mm long sections placed with central span of 765 mm. For the channel sections, tested sections had similar material properties to section C-W200T2.0 (Table 1) were used in the bending test under a pair of 3879 mm long sections placed with central span of 1293 mm. They had nominal dimensions as follows: a thickness of 2.0 mm, a depth of 255 mm, flange's width of 75 mm and lip length of 19 mm.

Lateral bracings were provided to prevent lateral torsional buckling in all FE models. The shape of initial geometric imperfections of 75% of CDF magnitude corresponding to 1.55t [28] was taken for the amplitude of initial imperfections. The elastic modulus E of 205 GPa was used. The inelastic part obtained from a model of literature, especially Hadarali and Nethercot [29] proposed the constitutive stress-strain model, in which a straight line with a constant slope of E/50 was used to model the plastic region of the stress-strain curve , where the elastic modulus E obtained from material tests. Full details on FE modelling could be found in [25].

In this paper, the measured material properties obtained from tensile specimen tests for flat and corners/bends were used in the FE models to accurately quantify the effects of geometry and the cold working induced from the cold roll forming process. Figs. 6(a-b) show both the measured engineering stress-strain curves and the true stress-strain curves, determined using the following equations:

$$\sigma_{true} = \sigma_{eng}\left(1 + \varepsilon_{eng}\right) \quad (6)$$

$$\varepsilon_{true}^{pl} = ln\left(1 + \varepsilon_{eng}\right) - \frac{\sigma_{eng}}{E} \quad (7)$$

where σ_{eng} and ε_{eng} are engineering stress and strain, respectively, based on the original gauge length of the specimens and the original cross-sectional area; and σ_{true} and ε_{true}^{pl} are the true stress and the true strain, respectively. Equations (6) and (7) could only be valid if stresses and strains are uniform over the gauge length, in other words, true stress and true strain does not have a negative slope. Therefore, the true stress-strain curves are only presented in Figs. 6a and 6b to the peak point of the engineering curves. 10 corners and bends were defined for the zed section, as shown in Fig. 6a, but only five corners and bends in the upper part of the section were calculated when assigning material properties as the others in the lower part were assumed to be the same due to symmetry. On the other hand, 12 corners and bends were defined for the channel section, as shown in Fig. 6b, but only six corners

and bends in the upper part of the section were calculated when assigning material properties as the others in the lower part were assumed to be the same due to symmetry.

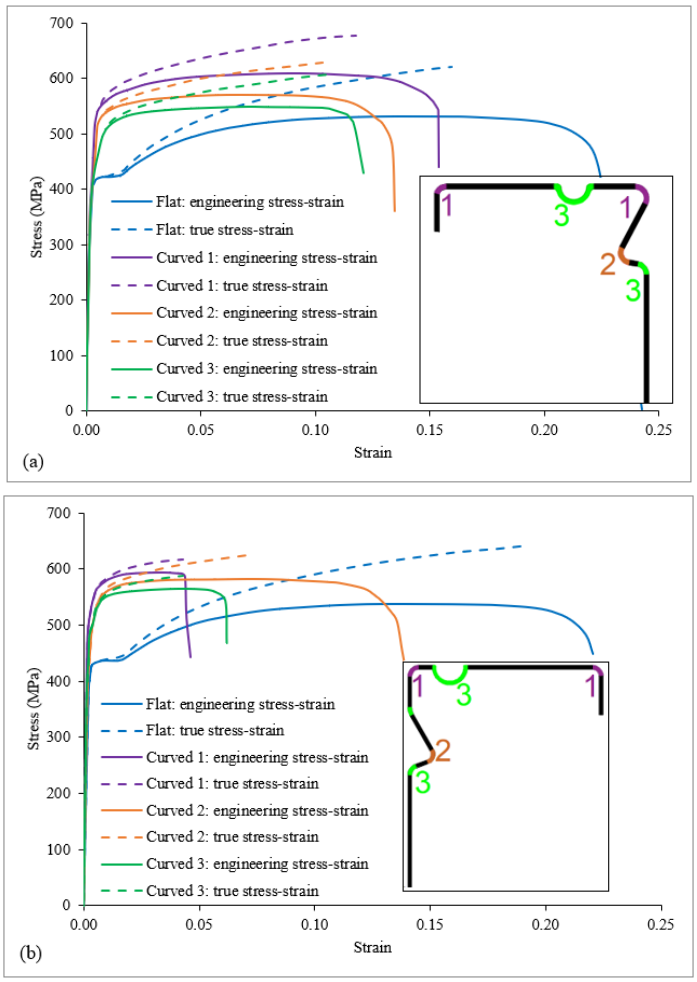

Figure 6: Typically measured stress-strain curves of the flat and curved specimens of (a) zed section Z-W200T2.0, and (b) channel section C-W200T2.0, which were used in the FE modelling as shown in Section 5.3.1.

4. Flexural strength optimization

This session study used the material properties obtained from the tensile test results in Section 4.3.1 in the FE models to optimize the buckling and ultimate bending strength of some selected channel and zed sections. The main purposes were to (1) accurately quantify both geometry and the cold working effects on the buckling and bending strength in the channel and zed sections with complex stiffeners, and (2) ultimately select and propose the optimal design of these channel and zed sections. Eventually, the effects of cold working on material properties at section's corners and stiffener bends on the flexural strengths could be evaluated from experimental data.

Fig.7 (a) shows a cross section and general dimensions for the channel sections which was the industrial UltraBeam™2 sections (Hadley Industries plc.), respectively, whereas Fig.8(a) shows a cross section and general dimensions for the zed sections which was the industrial UltraZED™2 sections (Hadley Industries plc.). The study goal was to find optimal design of the web and flange stiffeners' positions, shapes, sizes, and enhanced material properties at corners and stiffeners' bends, which enhance the section's buckling and ultimate bending strength, leading to an optimal design of the sections. The FE model developed and validated in [25] and in Section 3 of this paper was utilized for the optimization study. The sections together with their bending setup used in the experimental testing in [27] were defined as "reference section" and shown in Fig.7 (b) and Fig.8(b). The section height h and thickness t were fixed in the optimization study. The optimal cross-sectional shapes investigated in this paper, are optimized based on an optimization framework developed by the authors in the previous studies [26,30] for the purpose of producing more efficient and optimal design of CFS sections. The proposed optimization framework takes the buckling and ultimate strength of CFS sections as objective function. In this approach, a nonlinear finite element model was first developed for a referenced channel and zed sections subjected to four-point bending tests and these reference sections were then parameterized in terms of geometric dimensions and material properties using the DOE technique. The section distortional buckling and ultimate strength were determined using a response surface in the next step including the influences of the stiffener's size, location and shape, and material properties by the cold working at the section corners and stiffener bends. The geometric dimensions and material properties of optimized sections were then determined by Response surface design optimization. The new optimized sections were then applied loading up to failure to obtain ultimate bending strengths.

Fig. 7(b) shows the channel section without flange stiffeners, in which all dimension parameters are also presented, and Fig. 7 (c) presents the channel section with flange stiffeners. For the reference channel section, the values for h and t were taken as 170.1 mm and 1.6 mm, respectively. The position of the web stiffeners from the web-flange junctions are p_1 and p_2, the position of the peak of the web stiffeners in horizontal direction from the web-flange junction is p_3, the width of the edge stiffener is p_4, the radius of the section corners is p_5 and it was assumed that they had the same radius, the angle of rotation of the web stiffener are p_6 and p_7, the flange width is p_8, the position of the flange stiffener away from web flange junction is p_{15}, and the size of the flange stiffener (assuming the flange stiffener had a circular shape) are p_{16} and p_{17}.

Fig. 8(b) shows the zed section without flange stiffeners, in which all dimension parameters are also presented, and Fig.

8(c) shows the zed section with flange stiffeners. For the reference zed section, the values for h and t were taken as 170.1 mm and 1.6 mm, respectively. The position of the web stiffeners from the web-flange junctions are p_1 and p_2, the width of the edge stiffeners are p_3 and p_4, the radius of the section corners is p_5 and it was assumed that they had the same radius, the position of the peak of the web stiffeners in horizontal direction from the web-flange junction are p_6 and p_7, the angle of rotation of the web stiffeners are p_8 and p_9, the angle of rotation of the edge stiffeners are p_{10} and p_{11}, the width of flanges for the zed section without flange stiffeners are p_{12} and p_{13}, whereas the position of the flange stiffeners away from web flange junction for the zed section with flange stiffeners are p_{12} and p_{13}, the size of the flange stiffeners are p_{14} and p_{15}, and the width of flanges are p_{16} and p_{17}.

For the optimization target, the total length of the cross section was kept unchanged, that was “obtaining maximum strength of the section while maintaining the same weight”. new channel and zed sections were obtained when changing parameters relating to the stiffeners’ sizes, shapes and positions while considering enhanced material properties at corners and bends by the cold working effect. In these new sections, the material properties at the flat regions, corners and at the stiffeners’ bends were assumed to be the same.

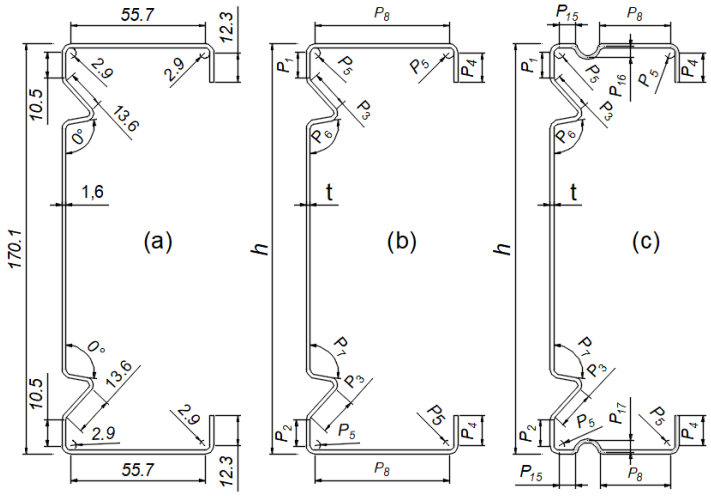

Figure 7: Dimension parameters in (mm) and definition of design variables of the channel cross section (a) reference section, (b) without flange stiffeners, and (c) with flange stiffeners

In the proposed FE approach, the three dimensional of the section beams was built first, allowing for the parameters to be parameterized (the size, positions, and shape of web stiffeners, the size of edge stiffeners and section corners, the positions of flange stiffener, and the size of flange stiffener). Next, the linear buckling analysis was carried out with the initial dimensions (i.e. the reference section dimensions) before conducting eigenvalue buckling analysis. Then, the nonlinear buckling analysis including material and geometry nonlinearity, initial geometric imperfections, and the cold working effect at section corners and stiffeners’ bends was conducted. The three analysis systems were linked allowed to share resources from the previous linear buckling analysis such as geometry, engineering data, and boundary condition type definitions. Finally, the response surfaces were calculated using the data from the parameterized Design Of Experiment process, and a multi-objective genetic algorithm was used to select the best design candidates. The detailed descriptions of the optimization approach could be found in [26].

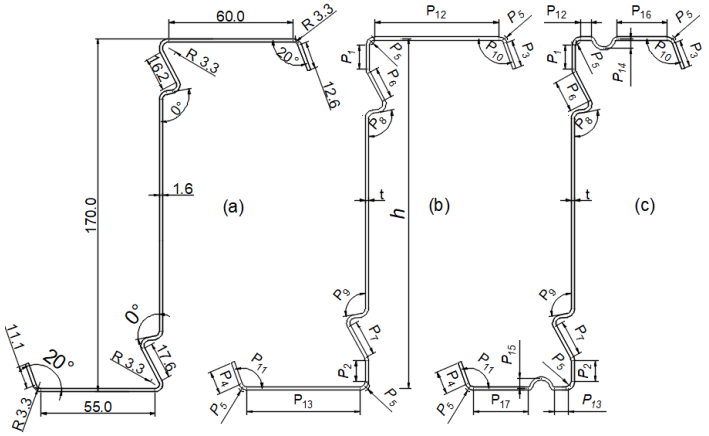

Figure 8: Dimension parameters in (mm) and definition of design variables of the zed cross section (a) reference section, (b) without flange stiffeners, and (c) with flange stiffeners

The cross-section namely “Standard” is a standard commercially available cross-section, which provided a basis for comparison. Reference (b) and (c) are the sections without and with flange stiffeners. Candidate 1-6 are optimized sections obtained based on different target objectives. Candidate 1 and 4 obtained when the ‘target’ was to minimize maximum developed stresses, Candidate 2 and 5 obtained when the ‘target’ was to maximize buckling, and Candidate 3 and 6 obtained when the ‘target’ was to minimize maximum developed stresses and maximize buckling in the cross-sections. In this optimization study, the tensile test results obtained from section 2.1 were used. The material properties of flat and corner/bend specimens of C-W200T2.0 were used for the reference zed section Z-W170T1.6 whilst the material properties of flat and corner/bend specimens of Z-W200T2.0 were used for the reference zed section.

5. Results and discussion

5.1 Tensile test results

A total of 96 tensile specimens obtained from 4 cross-sections was tested to determine the mechanical properties of the material. This included the 16 tensile specimens extracted from the pre-cold rolled sheet coils (virgin materials), 16 specimens extracted from the web of the

sections, 16 specimens extracted from the flanges of the sections, and 48 specimens extracted from the section corners and stiffener's bends. The thickness of the test specimens ranged between about 1 and 2 mm, while the corner radii ranged between about 2 and 5 mm. The measured yield strength of the section's corner and stiffener's bend material f_{yc} has been normalized by the yield strength of the virgin material $f_{y,mill}$ to indicate the level of strength enhancement due to corner and stiffener forming as (%), while in Figs. 10(a-b) are shown the ultimate tensile strength distribution for the same profiles.

From Figs. 9-10, it may be seen that the material properties of measured virgin material (sheet coil) and the flat specimens extracted from the complete sections are similar. An average increase in strength of around 1% to 4% over the virgin value was observed based on the limited results presented in this study which indicate modest levels of strength enhancement in the flat faces of web and flanges of the steel channel and zed sections during the cold roll forming process. These were consistent with results from previous studies [2,3]. However, due to work hardening that arises from plastic deformations induced during section-forming the mechanical properties of section corners and stiffener bends could significantly change.Compared to the flat specimens the yield and tensile strengths were increased by 17–29% and 5–15% in the curved specimens respectively, the percentage of elongation decreased by 40–84%. The cold working by the cold roll forming process produces a significant increase in the yield and tensile strengths and a decrease in ductility of the section corners and stiffener's bends. The effect of the cold working on the mechanical properties of web and flange specimens, however, was very small, compared to the amount of cold working in the curved locations so that it could be neglected.

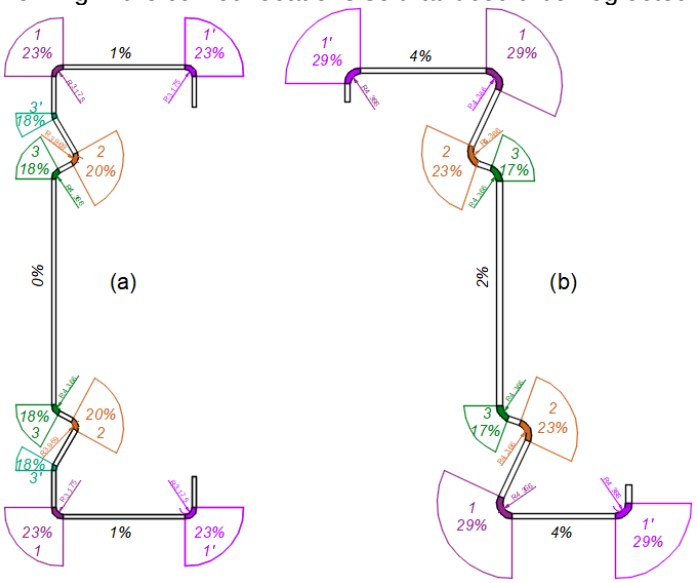

Figure 9: Yield strength enhancement in the sections due to cold roll forming (a) channel cross-section C-W200T2.0, and (b) zed cross-section Z-W200T2.0.

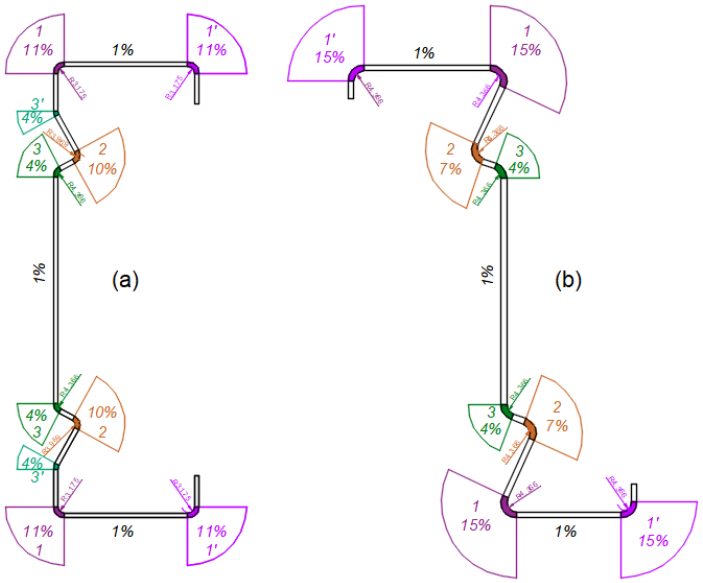

Figure 10: Ultimate strength enhancement in the sections due to cold roll forming (a) channel cross-section C-W200T2.0, and (b) zed cross-section Z-W200T2.0.

5.2 Comparisons of predictive models with measured increased yield stresses

Representative comparisons between the corner yield strengths determined from the experiments $f_{yc,test}$ against those obtained using the two different predictive models $f_{yc,pred}$, presented in terms of the predicted-to-test ratios, are shown in Table 2. The accuracy of the two different predictive models described earlier for the determination of the increased yield strength of section corner and stiffener bend materials extracted from the three locations of four cold-formed steel sections is assessed herein. Overall, it is observed that the section corner and stiffener bend yield strength may be significantly higher than that of the virgin material, with an average enhancement in yield strength of around 22% for the measured test data carried out in this study. Note that the strength enhancement in the flat faces of cold-formed steel sections (the results were shown in section 5.1) is typically relatively small due to the limited amount of cold-work induced in the flat parts during the roll-forming process.

For all the corner and stiffener bend regions, the results obtained from both predictive models the AISI Specification [12] and Gardner et al. [11], confirming that the yield strength of the materials have been considerably improved compared to the virgin sheet coil materials. As indicated in Table 2, the predictive model set out in the AISI Specification [12] provides relatively over predictions of $f_{yc,test}$, in terms of the average ($f_{yc,pred}$ / $f_{yc,test}$) by about 12%, while the model proposed by Gardner et al. [11] generally under-estimates $f_{yc,test}$ on the average by about 6%. Though the later method was calibrated based on

cold rolled hollow sections, the former [12] model is more widely used and is hence recommended for determining the corner yield strength of cold-formed steel sections when facing the lack of test data.
In this study, together with material properties obtained from tensile tests, material properties obtained from the AISI predictive model, which is used for predicting the yield strength of cold-formed sections and is based on the tensile material properties of the flat specimen cut from either the same cold-formed steel section or the virgin/sheet material, has been selected and used to account for the cold working effects.

5.3 FE modelling

5.3.1 Four-point beam bending test modelling validation

Further validation of FE models was carried out for four-point beam bending tests and compared with various experiments performed by Nguyen et al. [27] to understand the cold working effects on bending strength of the channel and zed sections. FE simulations were performed using both the measured material properties and the AISI specification calculated values for strength enhancement in the section corner and stiffeners bend regions. The FE model results were then compared with the four-point bending tests conducted in [27].

A comparison of ultimate moment capacity for beams with different span lengths is summarized in Table 3, where M_u, M_{uc} stand for ultimate moment capacity without and with the cold working effect, respectively. The ultimate moment capacities from experimental tests [27] and FEM and the ratios between two methods for each section are also presented in the Table 3. It shows the FE results were in an excellent agreement with the experimental results in achieving ultimate moment values.

Table 2: Comparison of yield strengths obtained by the proposed predictive models and representative test data for the 0.2% proof strength of curved regions of cold-formed sections ($f_{yc,pred}$ / $f_{yc,test}$).

Curved specimen location	t (mm)	R (mm)	$f_{yc,test}$ (MPa)	$f_{yc,pred}$ / $f_{yc,test}$	
				[12]	[11]
Z-W200T2.0-1	1.934	4.366	550	1.05	0.87
Z-W200T2.0-2	1.942	4.366	525	1.08	0.91
Z-W200T2.0-3	1.952	4.366	500	1.14	0.98
Z-W145T1.2-1	1.259	2.381	510	1.15	0.96
Z-W145T1.2-2	1.243	2.381	510	1.14	0.96
Z-W145T1.2-3	1.225	2.778	505	1.12	0.95
C-W200T2.0-1	1.994	3.175	540	1.14	0.98
C-W200T2.0-2	1.948	3.969	527	1.12	0.94
C-W200T2.0-3	1.964	4.366	515	1.13	0.94
C-W200T2.0-1	1.241	3.175	427	1.05	0.85
C-W200T2.0-2	1.242	1.984	421	1.16	0.98
C-W200T2.0-3	1.185	2.778	401	1.14	0.95
Average				1.12	0.94
St. dev.				0.035	0.039

Table 3: Ultimate moment capacities obtained from experimental tests and FE models. M_u, M_{uc1}, M_{uc2} stand for ultimate moment capacity without and with the cold working effect using both the measured material properties and the AISI specification calculated values, respectively.

Section types	Span length (m)	M_{test} (kNm)	FEM			M_{test}/ M_u	M_{test}/ M_{uc1}	M_{test}/ M_{uc2}
			M_u (kNm)	M_{uc1} (kNm)	M_{uc2} (kNm)			
Zed section	2.295	5.59	5.50	5.76	5.76	1.02	0.97	0.97
Channel section	3.879	30.06	28.83	29.75	29.75	1.04	1.01	1.01

It can be concluded from Table 3 that the cold working influence on bending strength of the channel section beam was small about 3% since the distortional buckling slenderness in the section was very high and the beam failed by distortional buckling stress before it reached its yield strength capacity. For the zed sections, the cold working effect was significant using both the measured material properties and the AISI specification calculated values about 5%, as the sections gained their full strength, and the generated stresses reached the plastic region.

5.3.2 Flexural strength optimization considering the cold working effect

The resulting cross-sectional shapes and comparison between flexural strength capacity with the cold working effects and without the cold working effects, using the measured material properties from the tensile specimen tests at flat, corner and stiffener bend regions, of the various optimal design candidate points are also shown in Fig. 11. The following observations were made from Figs. 11-12:

- The extent of improved distortional buckling and ultimate bending strength benefit obtained from geometry and the cold working effects was dependent on the cross-section shape and dimensions, and the

percentage area of the section corners and stiffeners' bends in the sections.

- Adding two longitudinal stiffeners to the web of the standard channel and zed sections (reference (b)) enhanced buckling considerably compared to the standard sections by 15% and 21%, respectively, whereas the ultimate moment capacity was noticeably improved by 2% and 8%, respectively. The cold working had noticeable effect by 2% on the reference section bending strengths.

- Having two longitudinal stiffeners in the web and one at the flanges of the standard sections (reference (c)) resulted in further enhancement in the buckling and ultimate moment capacity by 15% and 8% for the channel section, respectively, and by 21% and 17% for the zed section, respectively. The cold working had considerably more effect by around 6% due to further improved buckling load and increased bend regions in the sections.

- The optimized sections with two longitudinal web stiffeners in the web (Candidate 3) could provide with significant enhancement in the buckling of the channel sections due geometry effects which were about 100%, whereas it only considerably increased the ultimate moment capacity by 4% and extra 4% was also obtained in the ultimate moment capacity when the cold working effects were also considered. For the zed section, Candidate 3 gained significant increase in buckling, ultimate moment capacity without the cold working effects and with the cold working effects included by 110%, 17% and 23%, respectively.

- The Candidate 6 seemed to be the optimal solutions for both the channel and zed sections gained significant buckling, ultimate moment capacity without the cold working effects and with the cold working effects included by 84%, 13% and 20% for the channel section, respectively, and 105%, 17% and 23% for the zed section, respectively.

- The Candidate 6 also exhibited a considerably increased stiffness compared to the reference sections (as shown in Fig. 12) for both the channel and zed sections, which is a direct result of enhancement in the buckling due to the stiffeners delaying and mitigating the stiffness degradation. It is noted that the flange width of the design candidate 6 is less than that of the reference section as the stiffeners size was accounting for in the total developed length of the section.

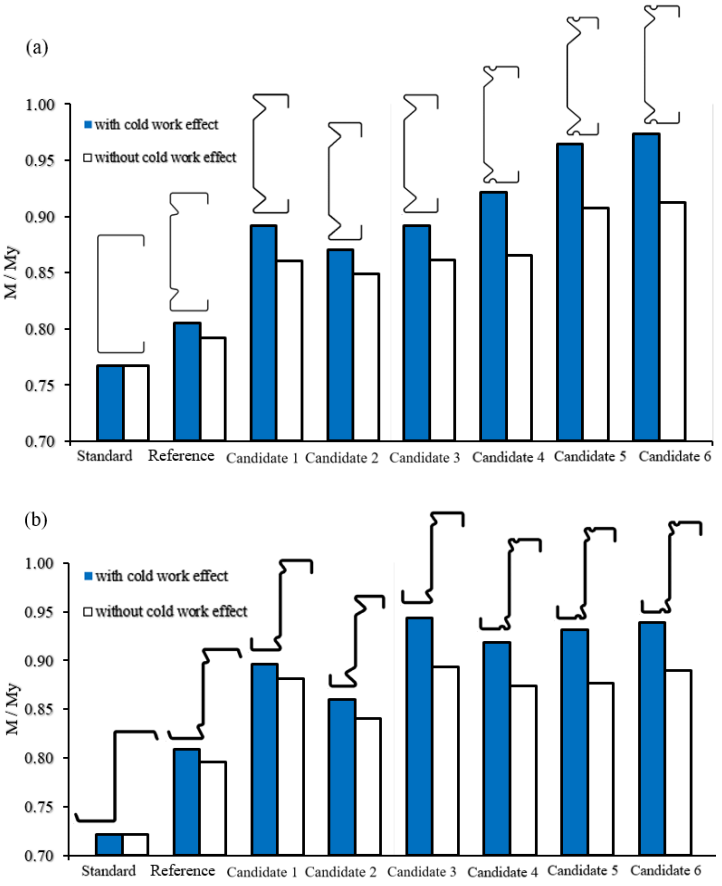

Figure 11: Ultimate bending strength to yield ratio with the cold working effects and without the cold working effects for (a) channel cross sections, and (b) zed cross sections.

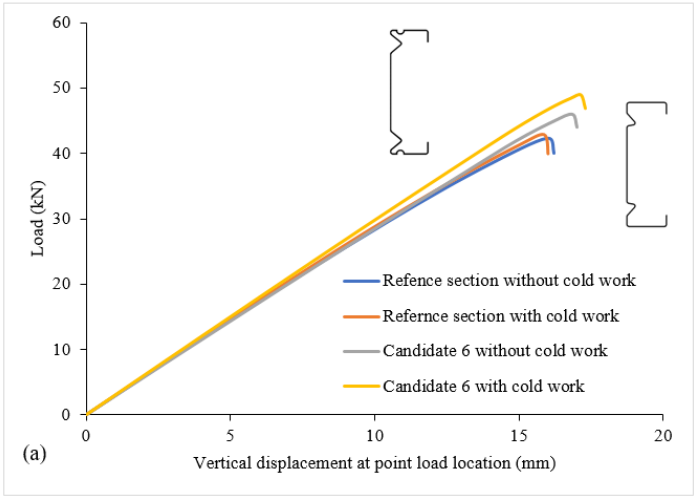

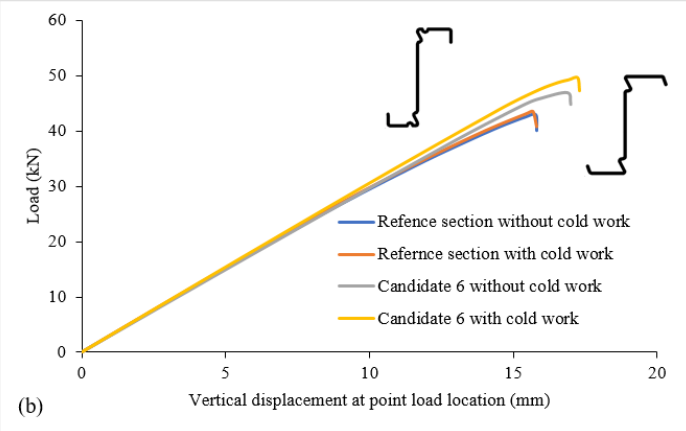

Figure 12: Load-displacement curves for the reference section and design candidate 6 results for (a) channel sections, and (b) zed sections.

It should be noted that the measured material properties carried out in this study may provide only a limited representation of the expected material properties for cold roll formed sections. Gardner et al. [31] performed a data collection from over 700 experimental stress-strain curves on cold-formed steels from the global literature and found the ratio (f_u/f_y) about 40%. Therefore, to gain more inside the cold working effects on bending strengths, new FE models were developed by considering different ratio of ultimate to yield tensile strength of the material (f_u/f_y) for the flat parts from the sections and the enhanced yield strength at section corner and stiffener bend regions determined based on the formulas in the AISI Specification [12]. The inelastic part obtained from a model of literature, especially Hadarali and Nethercot [29] proposed the constitutive stress-strain model, in which a straight line with a constant slope of E/50 was used to model the plastic region of the stress-strain curve , where the elastic modulus E obtained from material tests. In Figure 13, the (f_u/f_y) ratio is plotted versus the bending strength with the cold working effects (M_{uc}) normalized by (M_u) for the reference and optimized sections.

A comparison between the M_{uc} and M_u results indicates that the strength variation caused by the strain hardening of the material in the corner and stiffener bend regions had noticeable effect on bending strength of the reference channel and zed sections about 1% and 3%, respectively. The main reason for the low contribution of the strain hardening can be the higher distortional buckling slenderness and the relatively small area of the rounded corners compared to the total cross section area in the reference sections. On the other hand, by comparing the predicted bending strength M_{uc} and M_u of the optimised sections, it is shown that the cold working effects can have significant effects on the predicted flexural strength capacity (up to 8% and 7% variation for channel and zed sections, respectively) and it actually linearly increased the bending strength for different (f_u/f_y). This confirmed the fact that for accurately obtaining enhancement in the ultimate moment capacity of the section, the cold working effect had to be included in the FE models, especially in the sections that are less prone to buckling and have higher (f_u/f_y) ratio.

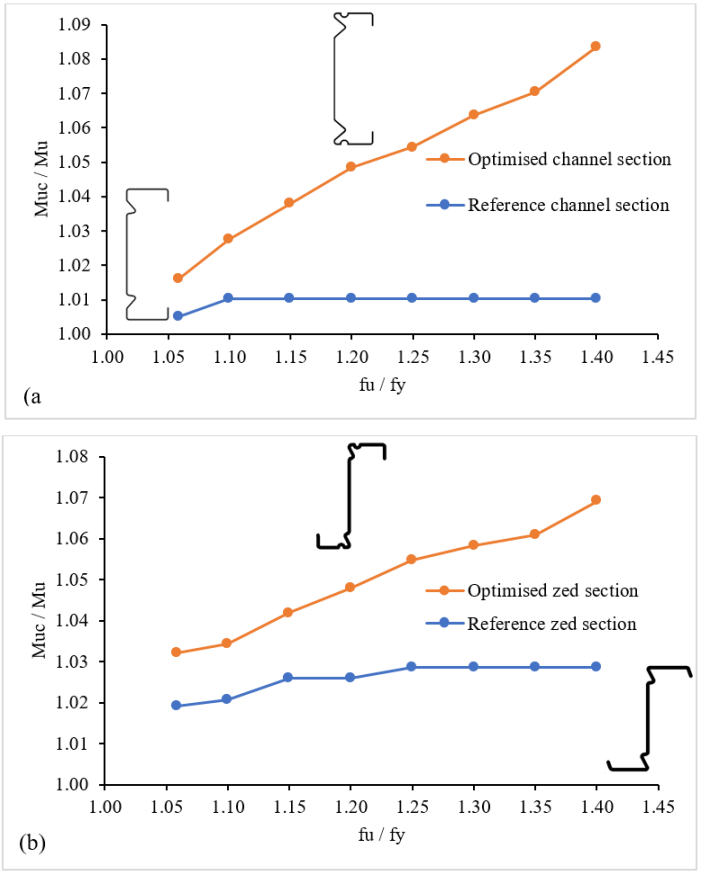

Figure 13: Bending strength enhancement due to cold roll forming process obtained for different ratios of ultimate tensile strength to yield strength of the materials for the reference and optimized sections (a) channel sections and (b) zed sections. The f_{yc} was determined using the North the AISI Specification [12].

6. Conclusions

In this paper, the influence of cold working effects on mechanical properties and flexural strength of the cold roll formed sections were studied by experimental testing and combined detailed Finite Element (FE) models and optimization. A material test programme on a total of four cold roll formed structural longitudinally stiffened sections, including two channel section and two zed sections was described. The results from tensile tests on 16 sheet coil specimens, 32 flat specimens, and 48 corner and stiffener bend specimens were presented. The cold working effect in

the corner and stiffener bend regions of cold roll formed sections was analyzed and the applicability of existing predictive models was evaluated. A practical method to obtain more efficient cold roll formed steel sections in bending using detailed (FE) modelling and Response Surface Optimization was presented. Four-point beam bending tests of the section was developed using the FE models. The models included material and geometrical nonlinear analysis with initial geometric imperfections and the cold working effects. This FE model was then utilized to optimize the buckling and flexural strength of the sections. Optimal cross-sectional shape of the longitudinally stiffened channel and zed sections was finally selected and proposed. Based on the results of this study the following conclusions were drawn:

1) The cold working had modest effect in material strength in the flat regions of cold roll formed steel sections by on average 2.5%, but significantly enhanced material strength in the corner and stiffener bend regions by on average 22%.; the results were compared with two predictive models and both models provided reasonable results.
2) The results revealed the efficiency of the adopted optimization approach to increase the bending strength of CFS sections. The ultimate moment capacity of the optimized CFS sections obtained from validated FE models were significantly higher than their standard and reference counterparts with the same amount of material used for both channel and zed sections. This improvement was more evident for the zed sections which they are less prone to distortional-global buckling failure mode.

3) The cold working effect in the corner and stiffener areas was insignificant on bending strength in the standard sections and only had a relevant influence at reference sections bending strength. The main reason for the low contribution of the cold working effects can be the higher distortional buckling slenderness and the relatively small area of the rounded corners compared to the total cross section area in the sections. On the other hand, the cold working effect significantly increased the stiffness and bending strength of the optimized sections up to 7% and 6% for the channel and zed sections, respectively. In the optimized sections, several parts of the cross-section presented an equivalent strain higher than the yield strain, so the increase of the yield strength in corner areas produced an increase of the flexural strength of the beams.
4) By considering both geometry and the cold working effects in the optimization process, optimal cross-sectional shape could be obtained with significant gain in distortional buckling and ultimate bending strength up to 84% and 20%, respectively, for the optimized channel section compared to the standard lipped channel, and up to 105% and 23%, respectively, for the optimized zed section compared to the standard lipped zed section using the same amount of material and the same height of the sections.

5) The optimal cross-sectional shape recommended to have two longitudinal stiffeners at the web placed as much close as possible to the web-flange junctions, one longitudinal flange stiffeners placed near the web flange junctions as much as possible, and the relative dimensions of the sections as proposed in this paper. The proposed shape could gain significant benefit from the geometry and the cold working effects.

8. Acknowledgments

We would like to acknowledge the University of Derby for providing the sponsor of this work [PGTA Studentship - E&T_14_PGTA_0717]. The tensile tests were carried out at the University of Sheffield.

References

[1] S. Afshan, B. Rossi, L. Gardner, Strength enhancements in cold-formed structural sections—Part I: Material testing, Journal of Constructional Steel Research 83 (2013) 177-188.

[2] M. Ashraf, L. Gardner, D. Nethercot, Strength enhancement of the corner regions of stainless steel cross-sections, Journal of Constructional Steel Research 61(1) (2005) 37-52.

[3] R.B. Cruise, L. Gardner, Strength enhancements induced during cold forming of stainless steel sections, Journal of constructional steel research 64(11) (2008) 1310-1316.

[4] L. Gardner, D.A. Nethercot, Experiments on stainless steel hollow sections—Part 1: Material and cross-sectional behaviour, Journal of Constructional Steel Research 60(9) (2004) 1291-1318.

[5] B. Rossi, Mechanical properties, residual stresses and structural behavior of thin-walled stainless steel profiles, University of Liège, Belgium, 2008.

[6] B. Rossi, S. Afshan, L. Gardner, Strength enhancements in cold-formed structural sections—Part II: Predictive models, Journal of Constructional Steel Research 83 (2013) 189-196.

[7] P. van der Merwe, J. Coetsee, G. van den Berg, The effect of workhardening and residual stresses due to cold work of forming on the strength of cold-formed stainless steel lipped channel sections, (1990).

[8] P. Van der Merwe, G. van den Berg, Prediction of corner mechanical properties for stainless steels due to cold forming, (1992).

[9] K.W. Karren, Corner properties of cold-formed shapes, Journal of the Structural Division 93(1) (1967) 401-433.

[10] N. Abdel-Rahman, K. Sivakumaran, Material properties models for analysis of cold-formed steel members, Journal of Structural Engineering 123(9) (1997) 1135-1143.

[11] L. Gardner, N. Saari, F. Wang, Comparative experimental study of hot-rolled and cold-formed rectangular hollow sections, Thin-Walled Structures 48(7) (2010) 495-507.

[12] AISI. North American specification for the design of cold-formed steel structural

members. AISI S100-16. Washington, DC; 2016.

[13] J. Bonada, M. Pastor, F. Roure, M. Casafont, Influence of the cold work effects in perforated rack columns under pure compression load, Engineering Structures 97 (2015) 130-139.

[14] Y.B. Kwon, G.J. Hancock, Tests of cold-formed channels with local and distortional buckling, Journal of Structural Engineering 118(7) (1992) 1786-1803.

[15] J. Ye, S.M. Mojtabaei, I. Hajirasouliha, Local-flexural interactive buckling of standard and optimised cold-formed steel columns, Journal of constructional steel research 144 (2018) 106-118.

[16] M. Jandera, L. Gardner, J. Machacek, Residual stresses in cold-rolled stainless steel hollow sections, Journal of Constructional Steel Research 64(11) (2008) 1255-1263.

[17] W. Quach, J. Teng, K. Chung, Effect of the manufacturing process on the behaviour of press-braked thin-walled steel columns, Engineering structures 32(11) (2010) 3501-3515.

[18] M. Jandera, J. Machacek, Residual stress influence on material properties and column behaviour of stainless steel SHS, Thin-Walled Structures 83 (2014) 12-18.

[19] V. Nguyen, C. Wang, D. Mynors, M. English, M. Castellucci, Compression tests of cold-formed plain and dimpled steel columns, Journal of Constructional Steel Research 69(1) (2012) 20-29.

[20] V. Nguyen, C. Wang, D. Mynors, M. Castellucci, M. English, Finite element simulation on mechanical and structural properties of cold-formed dimpled steel, Thin-Walled Structures 64 (2013) 13-22.

[21] V.B. Nguyen, D. Mynors, C. Wang, M. Castellucci, M. English, Analysis and design of cold-formed dimpled steel columns using Finite Element techniques, Finite Elements in Analysis and Design 108 (2016) 22-31.

[22] F. Wang, Numerical studies of residual stress in cold formed steel sigma sections, University of Birmingham, 2015.

[23] E. CEN, 1-3 Eurocode 3: Design of steel structures-Part 1-3: General rules-Supplementary rules for cold-formed members and sheeting, European Committee for Standardization, Brussels (2006).

[24] B.W. Schafer, The direct strength method of cold-formed steel member design, Journal of constructional steel research 64(7-8) (2008) 766-778.

[25] S. Qadir, V.B. Nguyen, I. Hajirasouliha, B. Cartwright, M. English, Optimal design of cold roll formed steel channel sections under bending considering both geometry and cold work effects, Thin-Walled Structures 157 (2020) 107020.

[26] S. Qadir, V. Nguyen, I. Hajirasouliha, B. Ceranic, E. Tracada, M. English, Shape optimisation of cold roll formed sections considering effects of cold working, Thin-Walled Structures 170 (2022) 108576.

[40] Y. Huang, B. Young, The art of specimen tests, Journal of Constructional Steel Research 96 (2014) 159-175.

[27] V.B. Nguyen, C.H. Pham, B. Cartwright, M. English, Design of new cold rolled purlins by experimental testing and Direct Strength Method, Thin-Walled Structures 118 (2017) 105-112.

[28] B. Schafer, T. Peköz, Computational modeling of cold-formed steel: characterizing geometric imperfections and residual stresses, Journal of constructional steel research 47(3) (1998) 193-210.

[29] M.R. Haidarali, D.A. Nethercot, Finite element modelling of cold-formed steel beams under local buckling or combined local/distortional buckling, Thin-Walled Structures 49(12) (2011) 1554-1562.

[30] S. Qadir, V. Nguyen, I. Hajirasouliha, B. Cartwright, M. English, Optimisation of flexural strength for cold roll formed sections using design of experiments and response surface methodology, Proceedings of the Cold-Formed Steel Research Consortium Colloquium, 20-22 October 2020 (2020).

[31] L. Gardner, X. Yun, Description of stress-strain curves for cold-formed steels, Construction and Building Materials 189 (2018) 527-538.